

The Subunit Structure and Dynamics of the 20S Proteasome in Chicken Skeletal Muscle*

Julia R. Hayter‡, Mary K. Doherty‡, Colin Whitehead§, Heather McCormack§, Simon J. Gaskell¶, and Robert J. Beynon‡||

We have succeeded in purifying the 20S core proteasome particle from less than 1 g of skeletal muscle in a rapid process involving two chromatographic steps. The individual subunits were readily resolved by two-dimensional PAGE, and the identities of each of the 14 subunits were assigned by a combination of peptide mass fingerprinting and MS/MS/*de novo* sequencing. To assess the dynamics of proteasome biogenesis, chicks were fed a diet containing stable isotope-labeled valine, and the rate of incorporation of label into valine-containing peptides derived from each subunit was assessed by mass spectrometric analysis after two-dimensional separation. Peptides containing multiple valine residues from the 20S proteasome and other soluble muscle proteins were analyzed to yield the relative isotope abundance of the precursor pool, a piece of information that is essential for calculation of turnover parameters. The rates of synthesis of each subunit are rather similar, although there is evidence for high turnover subunits in both the α (nonproteolytic) and β (proteolytic) rings. The variability in synthesis rate for the different subunits is consistent with a model in which some subunits are produced in excess, whereas others may be the rate-limiting factor in the concentration of 20S subunits in the cell. The ability to measure turnover rates of proteins on a proteome-wide scale in protein assemblies and in a complex organism provides a new dimension to the understanding of the dynamic proteome. *Molecular & Cellular Proteomics* 4:1370–1381, 2005.

Intracellular protein catabolism in eukaryotic cells is mediated by several specialized systems, of which the ubiquitin-proteasome system is probably the most active. In its physiologically active form, the 26S proteasome is a multimeric complex comprising 19S cap structures attached to either end of a barrel-shaped 20S core particle that contains the proteolytic machinery. Proteins are committed to degradation by attachment of a polyubiquitin chain to the ϵ -amino groups

of lysine residue(s). The polyubiquitin chain is then recognized by a 19S cap structure, which acts to unfold the protein chain and injects the polypeptide chain into the central core of the 20S subunit, wherein proteolysis takes place. The 20S proteasome has been isolated from Archaea, Eubacteria, and eukaryotes, consistent with an evolutionarily conserved mechanism for specific and specialized protein removal from the cell. The 20S core particle is barrel-shaped, formed from two α and two β rings each containing 7 α or 7 β proteins in an $\alpha 7\beta 7\beta 7\alpha 7$ configuration. The α and β subunits have masses typically ranging between 21 and 31 kDa; the entire 20S complex has a mass of approximately 700 kDa (1–3). Proteolytic activity in the 20S core is confined to the β rings, specificity is broad range and includes trypsin-like, chymotrypsin-like, and peptidylglutamyl activity, such that substrates are broken down into oligopeptides between 3 and 25 amino acids in length (4). The $\alpha 7\beta 7\beta 7\alpha 7$ structure is apparent in all 20S proteasome structures, ranging from the simplest structure isolated in *Thermoplasma* in which there are only single α and β proteins to the more complex eukaryotic structures, comprising seven distinct α and seven distinct β proteins. Additionally, further β proteins substitute for the catalytic core β proteins in the immunoproteasome (5–7).

We are studying mechanisms of protein degradation in avian skeletal muscle (8). The chicken offers a potent genetic and physiological model for regulation of muscle protein degradation. Lineages selected for meat production (broilers) grow at dramatically higher rates than those selected for egg production (layers) (9, 10), and previous data are consistent with the view that the higher rate of accretion of protein in broilers is predominantly a result of a diminution in rates of intracellular protein catabolism. Because the ubiquitin-proteasome system is considered to play a critical role in skeletal muscle protein breakdown (11, 12), we have characterized the 20S proteasome core particle from chick skeletal muscle. The 20S proteasome has previously been isolated from skeletal muscle of rat, rabbit, pig, cow, lobster, and chick (embryo and adult). These studies have predominantly focused on proteolytic activity and tissue-specific expression. Five β subunits from ostrich skeletal muscle have also been matched to human and bovine 20S proteins by virtue of N-terminal sequences (13). We therefore isolated the 20S proteasome from chicken skeletal muscle and identified each subunit using a

From the ‡Department of Veterinary Preclinical Sciences, University of Liverpool, Liverpool L69 7ZJ, United Kingdom; §Roslin Institute, Roslin BioCentre, Midlothian EH25 9PS, United Kingdom; and ¶Michael Barber Centre for Mass Spectrometry, Department of Chemistry, University of Manchester, Manchester M60 1QD, United Kingdom

Received, September 27, 2004, and in revised form, May 9, 2005
Published, MCP Papers in Press, June 19, 2005, DOI 10.1074/mcp.M400138-MCP200

combination of two-dimensional (2D)¹ electrophoresis, in-gel protein digestion, MALDI-TOF peptide mass fingerprinting (PMF), and *de novo* sequencing by MS/MS. We have been able to identify all 14 20 S subunits using these approaches.

One aspect of proteasome function that has not yet been addressed relates to the macromolecular dynamics, turnover, and plasticity of the proteasome itself. It is not clear whether the activity of the proteasomal machinery is present at sufficiently high levels as to always exceed the delivery of polyubiquitinated proteins. Relevant to this question is the rate of turnover of the proteasome subunits themselves. Is the proteasome turned over as a unit, and if so, by what mechanisms? Alternatively, is dynamic 20S (complete or partial) disassembly a prerequisite to turnover of individual subunits? To broach this question, we have used novel stable isotope-labeling protocols to assess the relative rates of turnover of the 14 individual subunits of the 20 S core particle.

EXPERIMENTAL PROCEDURES

Animals—Layer (ISA Brown) chicks were obtained immediately post-hatching and grown to 6 days on a synthetic diet with valine as the limiting amino acid (see below). Birds were fed *ad libitum* and were maintained on a 23-h light/1-h dark cycle. At day 6, the birds were switched to a “heavy” variant of the diet in which 50% of the ingested valine was present as the stable isotope [²H₈]valine. Valine was chosen as an essential amino acid, abundant in the chick proteome, that is also metabolically and chemically stable. Birds were culled up to 120 h of feeding with the stable isotope-labeled diet. The pectoralis (breast) muscle was excised and stored at -80 °C until required.

The diet comprised (g/kg): ground wheat, 750; soya oil, 40; cellulose, 30; dicalcium phosphate, 18; limestone, 15; vitamin and mineral mix, 5; salt, 3; choline chloride (50%), 1.5; arginine, 8.8; glycine, 6; histidine, 1.78; isoleucine, 5.15; leucine, 6.9; lysine, 8.75; methionine, 3.8; cystine, 2.2; phenylalanine, 3.75; tyrosine, 4; proline, 6; threonine, 5.75; tryptophan, 1.1; aspartic acid, 29; alanine, 20; glutamic acid, 20; valine (normal or deuterated), 5.55. The composition of the vitamin/mineral mix was designed to provide, per kg diet: vitamin A, 12,000 IU; vitamin D₃, 5,000 IU; vitamin E, 50 mg; vitamin K, 3 mg; thiamine, 2 mg; riboflavin, 7 mg; vitamin B₁₂, 15 µg; nicotinic acid, 50 mg; pantothenic acid, 15 mg; biotin, 200 µg; folic acid, 1 mg; zinc, 80 mg; copper, 10 mg; iodine, 1 mg; iron, 80 mg; manganese, 100 mg; selenium, 200 µg; cobalt, 500 µg. At 6 days, birds were switched to the heavy diet, in which 50% of the valine in the diet (that proportion added as crystalline amino acid) was replaced with [²H₈]valine (Cambridge Isotope Laboratories). The dietary changeover to the labeled diet was taken as *t* = 0 and samples were timed from this point.

Purification of the 20S Proteasome—The purification protocol was based upon previously published methods adapted for purification of the complex from large or smaller quantities of tissue (14–16). Chick skeletal muscle was mechanically homogenized using a domestic food processor in 1.5 volumes of buffer A (20 mM Tris, 20 mM KCl, 10 mM magnesium acetate, 2 mM DTT, 10% glycerol, pH 7.6). The soluble protein fraction was isolated by centrifugation at 30,000 × *g* for 30 min at 4 °C. The pellet was discarded, and the supernatant fraction was centrifuged again at 100,000 × *g* for 6 h. The supernatant

fraction was again discarded, and the pellet was washed carefully in fresh buffer, which was also discarded. The washed pellets were resuspended in 1 ml of buffer A (per pellet), pooled, and stored at -20 °C in 1.5-ml aliquots. For muscle from chicks fed a diet containing [²H₈]valine, the tissue (~5 g) was mechanically homogenized using a YSTRAL 10T homogenizer. For each gram of tissue, 1 ml of buffer B (20 mM MES, 50 mM NaCl, pH 6.0) was added, and the soluble protein fraction was isolated by centrifugation at 25,000 × *g*, 4 °C for 45 min.

Proteasome activity was measured by the release of 7-amino-4-methylcoumarin from *N*-succinyl-Ala-Ala-Phe-7-amido-4 methylcoumarin (Sigma-Aldrich). Aliquots of each fraction were incubated with an equal volume of reaction mixture containing 100 mM Tris (pH 7.5), 20 mM MgCl₂, 0.5 mM DTT, and 0.1 mM peptide substrate. The reaction was allowed to continue for 30 min at 37 °C and was stopped by the addition of 1 ml of 0.1 M sodium borate and 80 µl 20% (w/v) SDS. The product was measured at an emission wavelength of 440 nm ($\lambda_{\text{excitation}} = 380 \text{ nm}$) using slit widths for excitation = 5 nm, emission = 10 nm. The chromatography fractions containing peptidolytic activity (presumed, and subsequently demonstrated to be the 20S proteasome complex) were pooled and used for further analysis. Protein concentrations were determined using the Coomassie® Plus protein assay (Perbio Science UK).

Isolation of 20S Proteasome from Unlabeled Skeletal Muscle—The soluble protein isolated from the unlabeled muscle homogenate was loaded onto a 16/60 HiPrep Sephacryl S-300 column (120 ml, Amersham Biosciences) on a Duo-flow chromatography platform (Bio-Rad). The column was equilibrated overnight at 100 µl/min in 20 mM Tris, 20 mM KCl, 10 mM magnesium acetate, 2 mM DTT, 10% (v/v) glycerol, pH 7.6. A flow rate of 1 ml/min was used. Fractions (2.0 ml) were collected between elution volumes of 28 and 78 ml, and coincident fractions from three consecutive runs were pooled. The soluble proteins present in each fraction were initially separated by one-dimensional (1D), 12.5% (v/v) SDS-PAGE and stained using Coomassie blue. The fractions containing the 20S proteasome were identified using a fluorescent assay to detect the peptidase activity of the complex. These fractions were then pooled and stored at -20 °C. The pooled size-exclusion chromatography fractions (~60 ml) were loaded onto a Resource Q column (Amersham Biosciences) on the Duo-flow chromatography platform using multiple 5-ml loop injections. The column was equilibrated in 20 mM Tris, 20 mM KCl, 10 mM magnesium acetate, 2 mM DTT, 10% glycerol, pH 7.6, and bound proteins were eluted in a linear salt gradient (0–1 M NaCl) over 30 min. Fractions (1 ml) were collected from the final injection through to the end of the gradient. The proteins present in each fraction were separated by SDS-PAGE, and those containing the 20S proteasome, identified by peptidolytic activity, were stored at -20 °C.

Isolation of 20S Proteasome from Labeled Skeletal Muscle—To isolate the 20S particle labeled with [²H₈]valine, size exclusion chromatography on a BioSilect 250-5 column (Bio-Rad) was used for the initial chromatographic separation on the Duo-flow chromatography platform. Fractions (0.5 ml) eluting between 6 and 8 ml were pooled from 10 chromatography runs. These pooled fractions were then further resolved by cation exchange chromatography on a UNO S column (Bio-Rad) on the Duo-flow chromatography platform. The column was equilibrated with 20 mM MES, pH 6.0, and bound proteins were eluted using a linear salt gradient (0–1 M NaCl) over 30 min and collected in 1-ml fractions. Fractions containing the 20 S proteasome activity were pooled and stored at -20 °C.

2D PAGE—For the 20S proteasome isolated from normal chicken skeletal muscle, 100 µl of the anion exchange fraction containing the 20S complex (~65 µg protein) was TCA-precipitated, and the pellet was washed in ether. Once air dry, the pellet was resuspended in rehydration buffer. This sample was loaded onto 11-cm linear IPG

¹ The abbreviations used are: 2D, two-dimensional; PMF, peptide mass fingerprint(ing); 1D, one-dimensional; RIA, relative isotope abundance; MIDA, mass isotopomer distribution analysis.

strips, pH 3–10 (Bio-Rad), using overnight active rehydration, and the strip was focused using the Protean IEF system in accordance with the manufacturer's instructions (Bio-Rad). The focused strips were equilibrated in reducing equilibration buffer (6 M urea, 0.375 M Tris, pH 8.8, 2% (w/v) SDS, 20% (v/v) glycerol, 2% (w/v) DTT) for 15 min and then in an alkylating buffer (6 M urea, 0.375 M Tris, pH 8.8, 2% (w/v) SDS, 20% (v/v) glycerol, 2.5% (w/v) iodoacetamide) for a further 15 min before the second-dimension separation was performed in 12% gels using the Criterion gel system (Bio-Rad). For the 20S proteasome labeled with [$^2\text{H}_3$]valine, 250 μl ($\sim 5 \mu\text{g}$ protein) of the ion exchange fraction containing the 20S complex was used. The same conditions were applied as described for the unlabeled sample. Proteins were initially visualized using Coomassie brilliant blue; silver stain was used secondarily to enhance fainter spots.

PMF—A gel plug containing the protein of interest was excised from the gel with a fine glass pipette and transferred to a microfuge tube. To each tube, destain solution consisting of 25 μl of 50 mM ammonium bicarbonate, 50% (v/v) ACN was added and incubated at 37 °C for 20 min. This process was repeated until all the stain had been removed. A 10 mM solution of DTT (25 μl) was added to each plug and incubated at 37 °C. After 30 min, the supernatant was discarded, iodoacetamide (25 μl , 55 mM) was added to each tube, and incubation continued in the dark for 60 min. The gel was dehydrated using 25 μl ACN, and incubation at 37 °C was resumed for 15 min. The supernatant was removed from the dehydrated plug, which was allowed to air dry. Once dry, the gel was rehydrated with 50 mM ammonium bicarbonate (9 μl) containing trypsin (1 μl of 100 ng/ μl trypsin stock reconstituted in 50 mM acetic acid). After 30 min, 50 mM ammonium bicarbonate (10 μl) was added to each tube, and digestion was allowed to continue overnight at 37 °C. The reaction was halted by the addition of 2 μl of formic acid. In-gel digestion of silver-stained proteins was performed using the same protocol preceded by a silver destain step. The destain solution in this instance was 1:1 mixture of 30 mM potassium ferricyanide and 100 mM sodium thiosulphate (25 μl per gel plug) (17). When multiple gel plugs were excised from a single spot, the plugs were treated separately, and the peptides were pooled once overnight digestion was complete.

MS for PMF was conducted on a reflectron-equipped MALDI-TOF instrument (Waters). Samples were mixed in a 1:1 ratio with a saturated solution of α -cyano-4-hydroxycinnamic acid in ACN:water:TFA (50:49:1 (v/v/v)). Monoisotopic peptide masses in the mass range of 800–4000 Da were used in the database search. Using the MASCOT search engine the peptide masses were searched against the MSDB database, a composite nonidentical protein sequence database built from several primary source databases and with a weighted retention of entries from higher quality databases (18). The initial search parameters allowed a mass error of up to ± 250 ppm, a single trypsin missed cleavage, carbamidomethyl modification of cysteine residues, and oxidation of methionine. The taxonomic search space was restricted to Chordata, and there was no restriction regarding mass or pI.

De Novo Sequencing by MS/MS—All analyses were performed using the Q-ToFmicro (Waters). Peptides generated from an in-gel digest were first assessed by MALDI-TOF to ensure digestion had occurred. The supernatant from each in-gel digest was desalted using a C18 ziptip (Millipore), and the peptides were eluted in 10 μl of 50% (v/v) ACN 1% (v/v) formic acid. Samples were introduced by static nanospray from metal-coated thin walled capillaries held at a typical potential of 1000 V. An initial mass spectrum was collected between m/z 350 and 1500 from which multiply charged ions were identified as candidates for MS/MS from their natural isotope envelope. A range of collision voltages (18–48 V) was used to optimize the fragmentation of the parent ions.

The product ion spectra were deconvoluted using MaxENT 3 software, and the peptide sequence was determined using the PepSeq software within the MassLynx package (Waters). Peptide sequences were searched against the protein database using NCBI protein-protein BLAST and the option to search for short nearly exact matches (www.ncbi.nlm.nih.gov/BLAST/). The taxonomy was limited to Vertebrata, the “expect” parameter was set to 20,000, and the word size to 2; no other parameters were limited. Where appropriate, peptide sequences were reconciled with proteins identified by the MALDI-TOF PMF.

Analysis of Proteasome Subunit Dynamics—To analyze relative turnover rates of the 20S proteasome subunits, we purified the complex from skeletal muscle derived from chickens that had been fed a diet containing deuterated valine. Subsequently, the extent of incorporation of stable isotope-labeled amino acid was determined by MALDI-TOF MS and mass isotope distribution analysis as described elsewhere (8). Briefly, soluble chicken proteins were separated by SDS-PAGE and five proteins, readily isolated on 1D SDS-PAGE, were subjected to in-gel trypsin digestion. The relative isotope abundance (RIA) of the precursor pool was calculated from peptides derived from these proteins and containing two or three valine residues. Once the RIA of the precursor pool was established, this parameter is constant for that entire tissue, and thus it was possible to calculate the relative rates of synthesis of each proteasome subunit.

RESULTS AND DISCUSSION

Identification of 20S Proteasome Subunits—The 20S proteasome complex was isolated from ~ 200 g of chicken pectoralis muscle by ultracentrifugation followed by two orthogonal dimensions of chromatography, yielding ~ 0.75 mg of protein, predominantly consisting of the 20S complex. As the 20S complex comprises 14 proteins all with a mass in the 20- to 30-kDa range, it was not possible to resolve these by 1D SDS-PAGE, necessitating a 2D PAGE separation. The predicted pI range for the human 20S subunits is 4.6–8.7. It was assumed that the chicken proteins would fall into a similar range, and therefore linear focusing strips of pH 3–10 were used for the separation (Fig. 1). A total of 16 strongly staining spots between 20 and 30 kDa were in evidence, in excess of the 14 core 20S polypeptide chains. Less clearly defined spot trains were also evident for a number of spots; these are likely to be post-translationally modified variants.

The major protein spots were identified by “bottom up” proteomics. Peptides were generated by in-gel tryptic digestion of the Coomassie-stained protein gels. Although the first assembly of the chicken genome sequence has now been announced (www.genome.gov/11510730), the protein databases derived therefrom are incomplete, and it was relatively difficult to obtain good identifications for each subunit by MALDI-TOF PMF alone. Good quality MALDI-TOF spectra were obtained for each of the proteins (data not shown); however, only seven of the subunits ($\alpha 2$, $\alpha 3$, $\alpha 4$, $\alpha 6$, $\beta 2$, $\beta 3$, and $\beta 5$) could be identified by PMF (Table I). Four of these seven ($\alpha 4$, $\alpha 6$, $\beta 2$, and $\beta 5$) matched to published chicken proteasome subunit sequences (we have used the subunit numbering scheme proposed by Baumeister *et al.*; see Refs. 1 and 2 for a complete cross-reference to different subunit designations). The peptides in the MALDI-TOF spectrum

FIG. 1. Purification of chicken muscle 20S proteasome. The 20S proteasome was purified from chicken skeletal muscle by a combination of size exclusion and strong anion exchange chromatography. The complex thus isolated was resolved by 1D and 2D gel electrophoresis. All 14 core particle subunits were identified by a combination of MALDI-TOF PMF and MS/MS/*de novo* peptide sequencing.

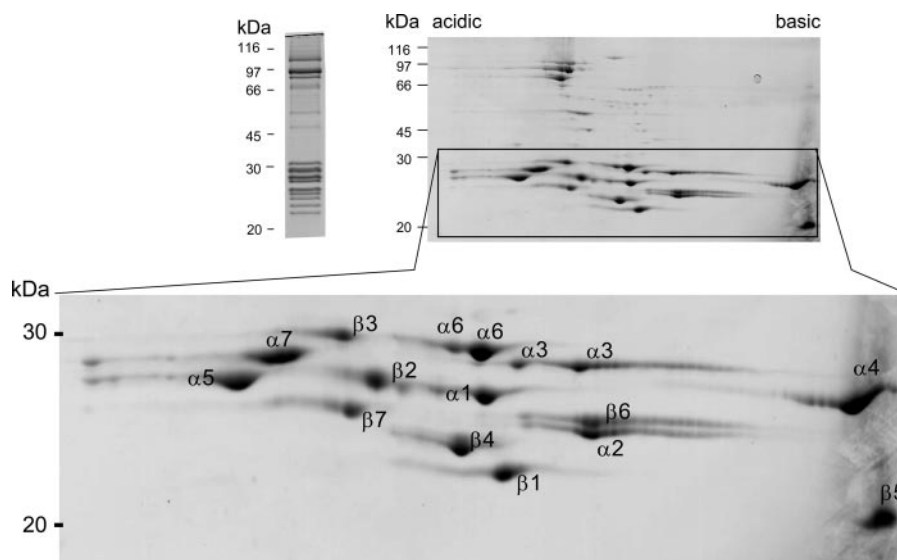


TABLE I

Identification of chicken 20S proteasome proteins by MALDI-TOF MS

The in-gel tryptic digests from the major spots were analyzed by MALDI-TOF and the PMF used to search the MSDB database using the MASCOT search tool. Seven peptide maps were matched to known 20S subunits, four from chicken (AF027978 NID, S30539, BAC76008, and JC5510) and three by cross-species matching (PSA2_human, SNHUC9, and S40468). Each bar is a single tryptic peptide. Shaded bars indicate those matched by PMF, and cross-hatched areas define additional peptides determined by LC-MS/MS and matched to the same proteins.

Protein	MASCOT Hit	Peptide map	Coverage (%)
$\alpha 2$	PSA2_human Proteasome subunit alpha type 2 (EC 3.4.25.1) - human		24
$\alpha 3$	SNHUC9; proteasome endopeptidase complex (EC 3.4.25.1) chain C9 - human		46
$\alpha 4$	JC5510 proteasome endopeptidase complex (EC 3.4.25.1) alpha chain - chicken		52
$\alpha 6$	O42265 : - proteasome alpha type 1 - chicken		52
$\beta 2$	Q7ZT63 proteasome subunit Z - chicken		30
$\beta 3$	S40468 proteasome subunit RC10-li - rat		30
$\beta 5$	P34065 proteasome endopeptidase complex (EC 3.4.25.1) chain C1 - chicken		43

matched between 24 and 52% of the intact protein sequence. Two subunits ($\alpha 3$ and $\alpha 6$) were identified in both a major and a minor spot; in both instances, the minor variants were more acidic, which would be consistent with a post-translational modification such as phosphorylation or deamidation. For $\alpha 3$, this would be in keeping with previous observations in other species (19, 20).

The PMF generated for subunit $\beta 2$ covered a relatively low proportion of sequence for this protein, matching seven peptides to SwissProt entry Q7ZT63. Tryptic peptide 7–8 (missed cleavage of K/D) has a predicted molecular weight of 2077.37 and sequence (K)TGTTIAGVVF~~K~~DG~~V~~LGADTR, which is not present in the MALDI spectrum. However, the second most intense peak in this spectrum is a peptide of mass 1918.05 Da, which is predicted by the sequence TTIAGVVF~~K~~DG~~V~~LGADTR, a sequence that has also been confirmed by nano-spray MS—S (see later). This is consistent with this peptide being the N-terminal residue of the mature subunit, exposing the catalytic threonine residue, after cleavage at the TG/TT site, a common β subunit activation site (21). For the remaining subunits identified by PMF, the coverage observed was variable (Table I). The fingerprints obtained for subunits $\alpha 2$ and $\alpha 3$ both matched to the equivalent human protein, but whereas the coverage for $\alpha 3$ was 46% for $\alpha 2$ this was only 24%. The majority of the peptides matched were toward the N terminus of each protein, suggesting that the subunits sequences were conserved at this end of the protein with variable regions located at the C termini.

Although PMF can give unequivocal identification of proteins recovered from a polyacrylamide gel, the confidence in the assignment is greatly enhanced if sequence data can also be acquired. We therefore used MS/MS to support the initial identifications and complete the characterization of the

chicken 20S proteasome (Table II). Each in-gel tryptic digest was desalted and concentrated using C18 ziptips (Millipore) prior to analysis of the peptide mixture using static nanospray. Candidate multiply charged ions were identified from a survey spectrum collected from 350 to 1500 Th, and for each spot several multiply charged ions were fragmented and sequenced. Sequence tags, ranging from short tracts of sequence to sequence runs of over 20 amino acids resulted in the identification of all 16 spots, confirming the MALDI-TOF data obtained previously. Twelve of the 14 proteins were identified by sequence data from multiple peptides (Fig. 2). For example, the peptide $[M+H]^+ = 2041.17$ Th observed in the PMF tentatively matched as the chick homologue of rat proteasome subunit $\alpha 2$ was partially sequenced from the triply charged ion $([M+3H]^{3+} = 681.05$ Th). The sequence LAAVAAGAPSVG~~I~~K matched to the rat $\alpha 2$ sequence apart from the substitution VAAGA, which in the rat is VAGGA, a conservative Ala to Gly substitution.

Human subunit $\alpha 7$ undergoes N-terminal processing with the loss of the N-terminal methionine and subsequent N-acetylation of the underlying serine residue (22). We have obtained very good evidence that the same modification is a feature of the chicken sequence. The chick EST database (chick.umist.ac.uk) contains multiple entries for partial sequences of subunit $\alpha 7$. The N-terminal sequence of the chick sequence is identical to the sequences of the equivalent subunit from other vertebrates, including mouse, rat, human, and *Xenopus*. One peptide derived from the spot corresponding to $\alpha 7$ $([M+H]^+ = 1959.9$ Th) was present in the MALDI-TOF spectrum and was also sequenced as the doubly charged ion $[M+2H]^{2+}$ (980.7 Th) ion by MS/MS. Although the fragmentation pattern permitted recovery of a short sequence tag (ASTFSxxGR), this was more than adequate to confirm

TABLE II
Proteasome subunit nomenclature and identification criteria

The subunit designation of Baumeister *et al.* (1) has been used in this article. Each subunit was identified by PMF to chicken proteasome subunits or by PMF from heterologous species. All nonchicken matches were confirmed as proteasome subunits by MS/MS *de novo* sequencing. The symbol *J* is used to indicate ambiguity between leucine and isoleucine.

Subunit	PMF identification (MOWSE score/significance threshold)	MS/MS identification	Sequence tag matched to	Predicted pI (approx.)	Predicted M_r (approx.)
$\alpha 1$		NQGGJTSVAVR	PSA6_human (P60900)	6.70	27
$\alpha 2$	PSA2 human, C3 (50/52), human	JVQJEYAJAAVAAGAPSVGJK	PSA2_rat (P17220)	7.10	26
$\alpha 3$	SNHUC9 chain C9 (74/67) human	JJDEVFFSEK	PSA4_human (P25789)	7.60	29
$\alpha 4$	JC5510 α chain (121/67), chick	JJTSPEEJEKYVAEJEK	PSA7_chick (JC5510)	8.90	28
$\alpha 5$		QSSJQEVYHK	PSA5_mouse (Q9Z2U1)	4.80	26
$\alpha 6$	AAC16604 (110/67), chick	HJGJSJAGJTADAR	PSA1_chick (O42265)	6.10	29
$\alpha 7$		AVENSSTAJGJR	PSA3_mouse (O70435)	5.40	28
$\beta 1$		TTTGSYVANR	PSB6_mouse (Q60692)	5.00	25
$\beta 2$	Q7ZT63 subunit Z (62/70), chick	TTJAGVVF K DG V VJGADTR	Q7ZT63 chick	6.00	29
$\beta 3$	S40469 RC10-li, rat	JYJGJAGJATDVQTVAGR	PSB3_rat (P40112)	6.20	23
$\beta 4$		EJSPTAAANFTR	PSB2_mouse (Q9R1P3)	7.00	23
$\beta 5$	S30539 chain C1 (188/65), chick	RVSSHDVAGJHDGYGG	PSB5_chick (P34065)	9.00	22
$\beta 6$		VYSFDPVGSYQR	PSB1_rat (P18421)	7.50	26
$\beta 7$		VJAADxxGSYGSJAR	PSB4_rat (P34067)	6.90	29

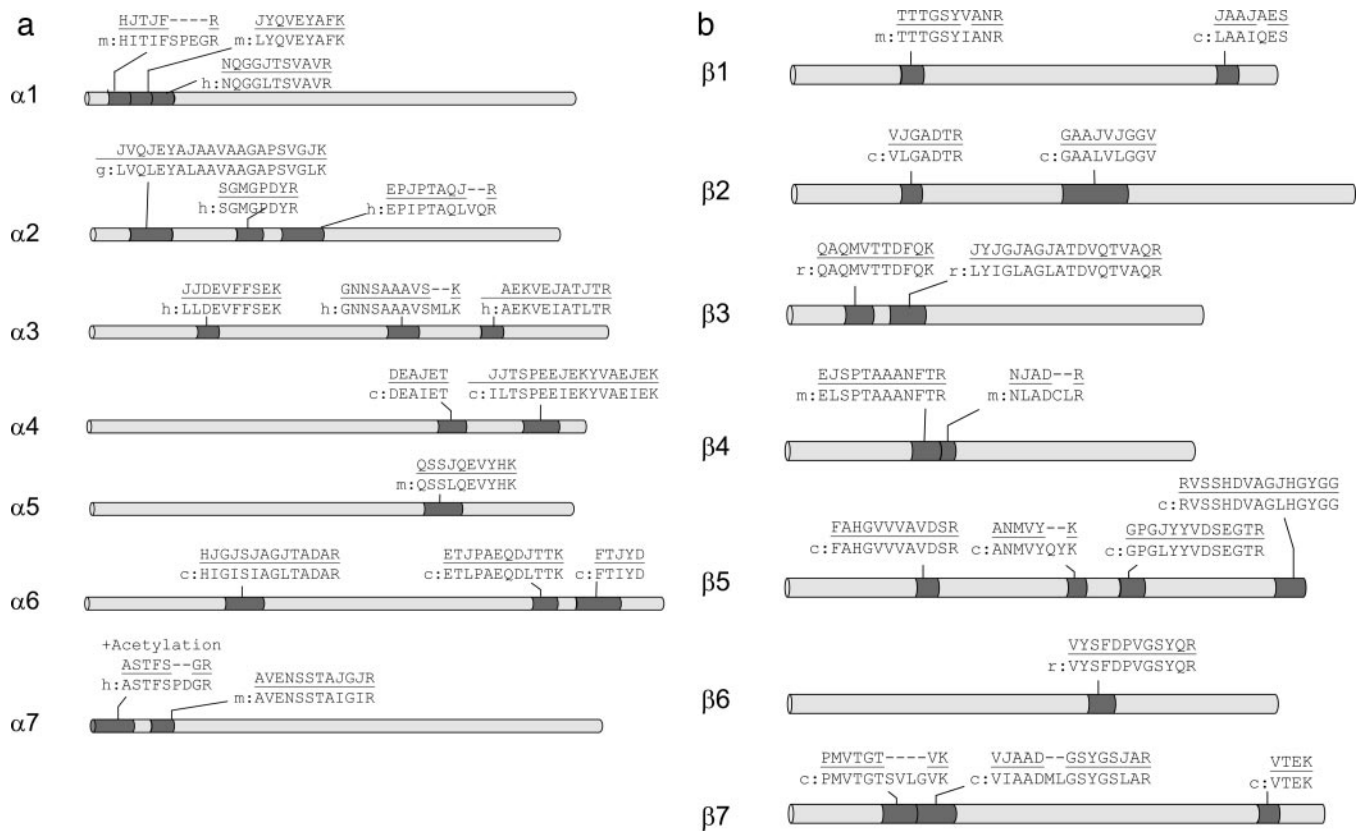


FIG. 2. Identification of chicken 20S proteasome subunits by nanospray MS/MS and *de novo* peptide sequencing. The in-gel digests from the 20S proteasome resolved by 2D gel electrophoresis were desalted using C18 ziptips and analyzed by static nanospray and MS/MS on a Q-TOF micro mass spectrometer. Protein sequences (*top line* of each sequence pair) were obtained by manual interpretation of the product ion spectra and used to search vertebrate databases using BLAST (www.ncbi.nlm.nih.gov/BLAST) The data shown here are representative of the sequence data obtained; for matches where chicken (c) proteins were not available the nearest sequence match was used; r, rat; m, mouse; h, human. Peptide sequencing by MS/MS on a Q-TOF instrument cannot discriminate isoleucine and leucine, thus the code *J* was used to represent these isomeric residues. A *hyphen* indicates that we were unable to determine the amino acid residue.

that this peptide was the N-terminal sequence of subunit $\alpha 7$. The mass of this peptide (1958.9 Da) is identical to that for the *des*-Met-, N-acetylated N-terminal trypsin peptide of $\alpha 7$ and provided strong confirmation that in the chicken this subunit is modified post-translationally at the N terminus in the same way as in the human proteasome.

All of the chicken 20S subunits were therefore identified and located on the 2D gel. This permitted comparison of the relative mobilities of the equivalent subunits in chicken and in human (23, 24). With the caveat that the 2D gel methodologies were not exactly comparable, the overall electrophoretic migration maps were remarkably similar (Fig. 3). The one striking discrepancy was subunit $\beta 1$, which migrated to a position corresponding to a much lower pI value in the 2D gel of the human proteasome. This implies that the overall charge distribution between the different proteasome subunits is largely conserved. The dramatically different mobility of this subunit in the two species is surprising and may have functional consequences. At this time, however, there is no full length cDNA sequence for chicken $\beta 1$, nor does a BLAST search against the current iteration of the chick genome elicit a full length sequence, and this

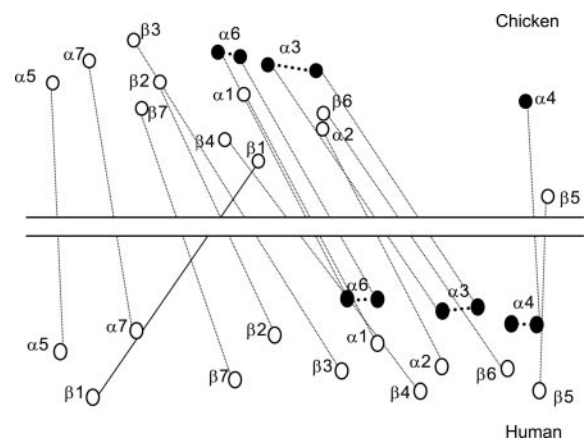


FIG. 3. Comparison of chicken and human 20S proteasome subunits resolved on 2D PAGE. The purified chicken 20S proteasome was resolved by 2D gel electrophoresis, and the location of each subunit was identified by MS. The location map was compared with the equivalent map for the human proteasome. Identical subunits are linked by *light dotted lines*, and where there are known post-translational modifications associated with specific peptides these are also linked by *bold dotted lines*.

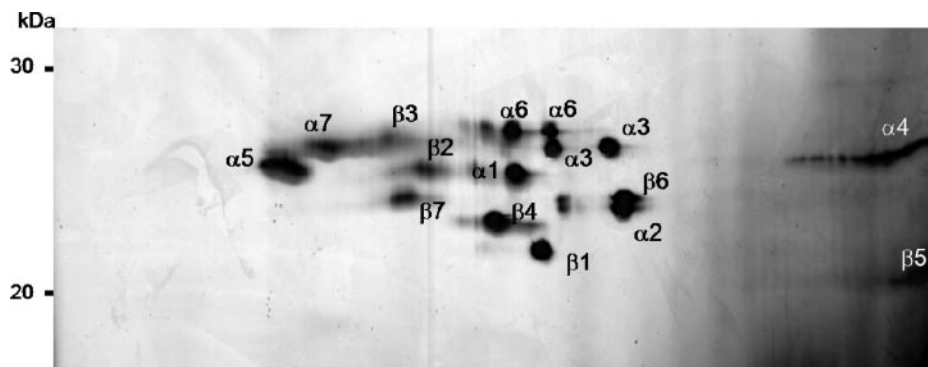
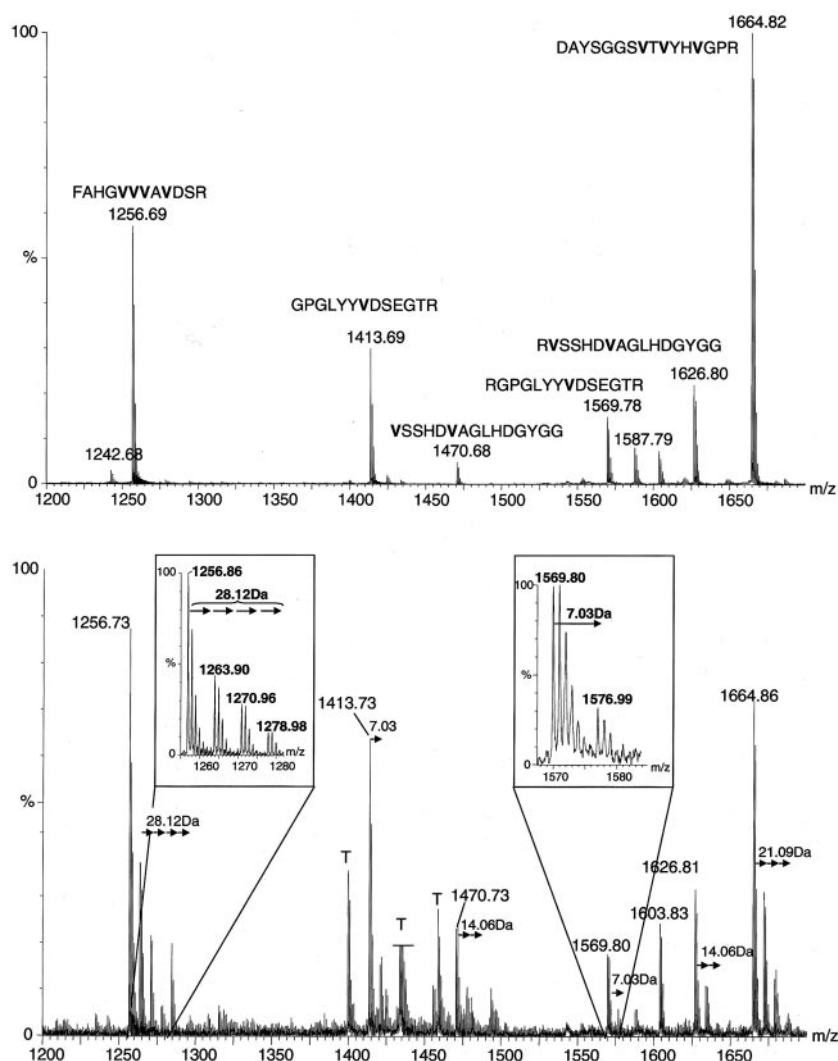


FIG. 4. **Chicken 20S proteasome purified from birds fed stable isotope-labeled valine.** The 20S proteasome was purified from birds that had been fed a diet comprising [²H₈]valine at a RIA of 0.5. Because of the limitations of the material (typically less than 0.5 g of muscle), it was necessary to devise a new purification protocol based on size exclusion and cation exchange chromatography. The purified proteasome was resolved by 2D electrophoresis and silver stained to reveal the subunit pattern.

FIG. 5. **Stable isotope labeling *in vivo* of chicken proteasome subunits.**

Chicks were fed a diet containing [²H₈]valine for 120 h, at which time the 20S proteasome was purified by sequential chromatographic steps. MALDI-TOF MS of an in-gel tryptic digest of each subunit was used to define the relative intensities of the unlabeled and labeled peptide variants. Representative spectra are shown for unlabeled (*top*) and labeled (*bottom*) variants of the chick β₅ subunit. The *inset panels* indicate the fine detail of the labeling pattern for a tetravaline peptide (unlabeled *m/z* 1256.8Th) and a monovaline peptide (unlabeled *m/z* 1569.8Th). Tryptic autolysis products are denoted *T*.



must therefore remain unresolved at present. However, a comparison of properties of the two proteasomes might elucidate an outcome of this difference in the β₁ subunits. Two 20S protea-

some subunits (α₃ and α₆) migrated as a pair of protein spots that differed along the IEF axis, consistent with a charge modifying post-translational modification. Interestingly, a similar be-

havior has been noted for the equivalent human 20S subunits. Furthermore, although less clearly defined, the $\alpha 4$ subunit also shows evidence of a “charge train,” and again this is a feature of the equivalent human subunit.

Relative Turnover of 20S Proteasome Subunits—We have developed stable isotope-based methods to determine relative and absolute turnover rates of individual proteins on a proteome-wide scale (8, 25). In brief, a diet fed to the birds was supplemented with [$^2\text{H}_8$]valine. Valine is an abundant amino acid in the chicken proteome, comprising ~6% of the amino acids. We therefore had the reasonable expectation that all 20S subunits would be labeled by incorporation of stable isotope-labeled valine. Furthermore, the relative rate of incorporation would indicate the relative rates of synthesis of the individual subunits. However, because the precursor pool was incompletely labeled, it was necessary to assess the RIA of the precursor pool from mass isotopomer distribution analysis (MIDA) of peptides containing multiple valine residues (stable isotope labeled or heavy (H) and unlabeled or “light” (L) (8), wherein the equations are derived). For example, for a trivaline peptide, the intensities of single labeled (L_2H) and doubly labeled peptide (LH_2) variants yield the relative isotope abundance thus:

$$RIA = \frac{I_{LH_2}}{I_{L_2H}} \left(1 + \frac{I_{LH_2}}{I_{L_2H}} \right) \quad (\text{Eq. 1})$$

where I_{LH_2} is the peak intensity of the peptide containing two labeled valine residues and I_{L_2H} is the peak intensity of the peptide containing a single labeled valine residue. From the value of RIA, it was then possible to measure the rate of turnover of each subunit from monovaline peptides, expressed as the fraction of the subunit pool that was newly synthesized, F_N :

$$F_N = \frac{I_H}{(I_L + I_H) \cdot RIA} \quad (\text{Eq. 2})$$

where I_H is the intensity of the labeled peptide and I_L is the intensity of the unlabeled peptide.

We could therefore assess the relative rates of turnover of all 14 of the 20S core proteins. The 20S particle was purified from birds that had been administered a diet containing [$^2\text{H}_8$]valine for up to 120 h. Because the quantity of tissue obtained from birds labeled in this way was small, it was necessary to modify the isolation of the 20S proteasome. A soluble protein fraction was resolved by size exclusion chromatography (fractionation range 5,000–100,000 Da), and fractions eluting near to V_0 contained peptidolytic activity toward *N*-succinyl-Ala-Ala-Phe-7-amido-4 methylcoumarin were further resolved using cation exchange chromatography. Fractions containing peptidolytic activity toward the same substrate were pooled and separated by 2D gel electrophoresis (Fig. 4). The spot pattern was virtually identical to that obtained from the bulk purification (Fig. 1).

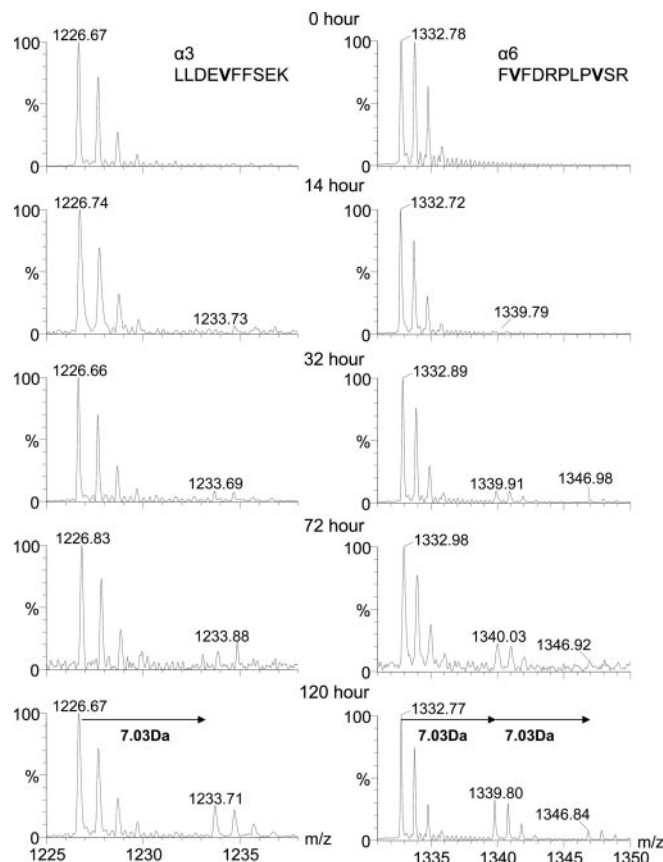


FIG. 6. Incorporation of stable isotope-labeled valine into proteasome subunits. Chicks were fed a diet containing [$^2\text{H}_8$]valine for 120 h. At 0, 14, 32, 72, and 120 h, the 20S proteasome was purified by sequential chromatographic steps. MALDI-TOF MS of an in-gel tryptic digest of each subunit was used to define the relative intensities of the unlabeled and labeled peptide variants. Representative data are shown for two peptides at m/z 1226.7 Th (subunit $\alpha 3$) and m/z 1332.8 Th (subunit $\alpha 6$).

This approach of using stable isotope-labeled amino acids to determine the turnover rates of individual proteins on a proteome-wide scale in an animal is not without complications. First, although the precursor used was [$^2\text{H}_8$]valine, we find that the increase in mass of a valine-containing peptide is $7.03n$ Da, where n is the number of valine residues in the peptide. We have noted this behavior previously in labeling studies with *Saccharomyces cerevisiae*, and we attribute this loss of mass to rapid transamination that leads to loss of the α -carbon deuterium. Indeed, we include this position in our labeling strategies as it indicates the equilibration of the precursor amino acid with the endogenous pool (26).

The complexity of the spectra derived from labeled proteasome subunits is revealed in the MALDI-TOF mass spectrum for the $\beta 5$ subunit. The spectrum was of high quality, although considerably more complex than that obtained with the unlabeled protein. Closer examination of the spectrum revealed that valine-containing peptides evidence more complex patterns, attributable to the incorporation of one or more than

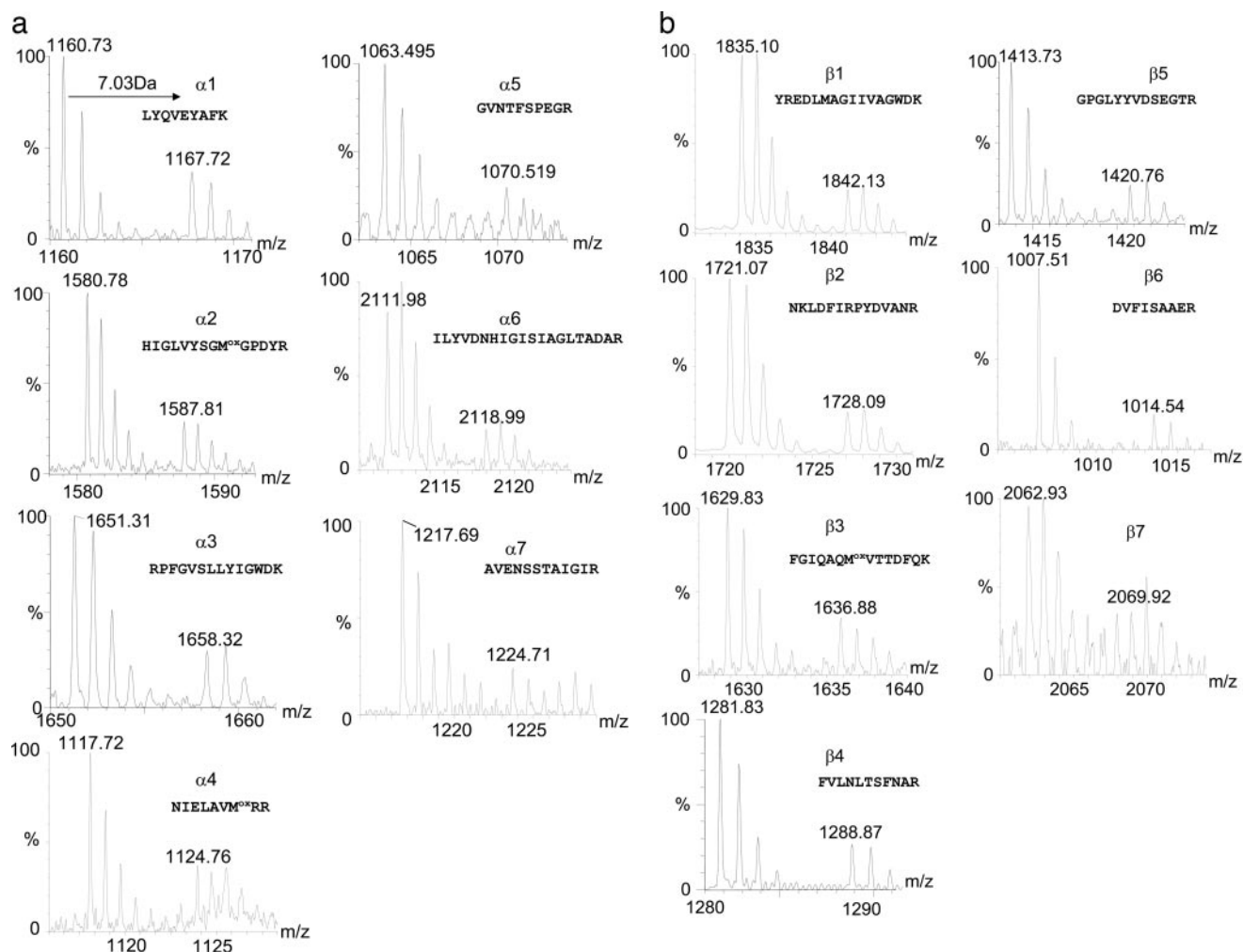


FIG. 7. Heavy-light valine peptide pairs identified for each of the 20S proteasome subunits. The peptide pairs were located in the MALDI-TOF spectrum for each protein and were distinctive due to the 7.03-Da mass difference between the light and heavy peaks for a single valine-containing peptide, after 120-h labeling. Mass differences of 14.06 and 21.09 Da were observed between the unlabeled and labeled peaks for two ($\beta 2$) and three ($\alpha 4$) valine-containing peptides with intermediates being located at intervals of 7.03 Da.

one residue (Fig. 5). The complexity of the pattern of labeling reflected the fact that the RIA was less than unity, and that the muscle would contain some unlabeled 20 S proteasome reflecting pre-existing material and the rate of degradation of that pool of unlabeled material. The pattern of the tetra-valine peptide FAHG⁴VAVDSR ($[M+H]^+$, 1256.73 Th) is particularly complex, yielding four discrete families of natural isotope distributions separated by 7.03 Da. These refer to the L_4 , HL_3 , H_2L_2 , and H_3L variants. The all heavy variant H_4 is not visible because it accounts for at most 0.35⁴ of the total labeled pool (equivalent to 1.5%). There is no evidence for incorporation of [²H₈]valine into proteins. However, the calculation of RIA or turnover rate is not dependent on the intensity of this peak, and it can be calculated by reference to other more highly labeled peaks.

To calculate the rate of turnover of the individual subunits, the 20S proteasome was isolated from muscle from a single bird at five different times over a 120-h labeling period. As

anticipated, stable isotope-labeled valine was incorporated into the 20S proteasome subunits, reflecting a combination of intracellular turnover and growth. Moreover, the labeling pattern was monotonic and is consistent with our previous experience of limited animal to animal variance (8). To illustrate the pattern of incorporation of label, the spectra corresponding to two peptides; monovaline T_8 (1226.67 Th) LLDEVFFSEK from subunit $\alpha 3$ and divalene T_{13} (1332.78 Th) FVFDRLPVSR from subunit $\alpha 6$, are displayed over the entire 120-h labeling period (Fig. 6). As the labeling time increased, there was a gradual appearance of a peptide corresponding to the incorporation of a single valine residue. For the divalene peptide, the peptide corresponding to two stable isotope-labeled valine residues was of lower abundance and was not readily apparent until at least 32 h of labeling. Accurate measurement of the relative turnover rates of the proteasome subunit required that the peaks corresponding to each labeled/unlabeled peptide were in an area of the mass spectrum with a

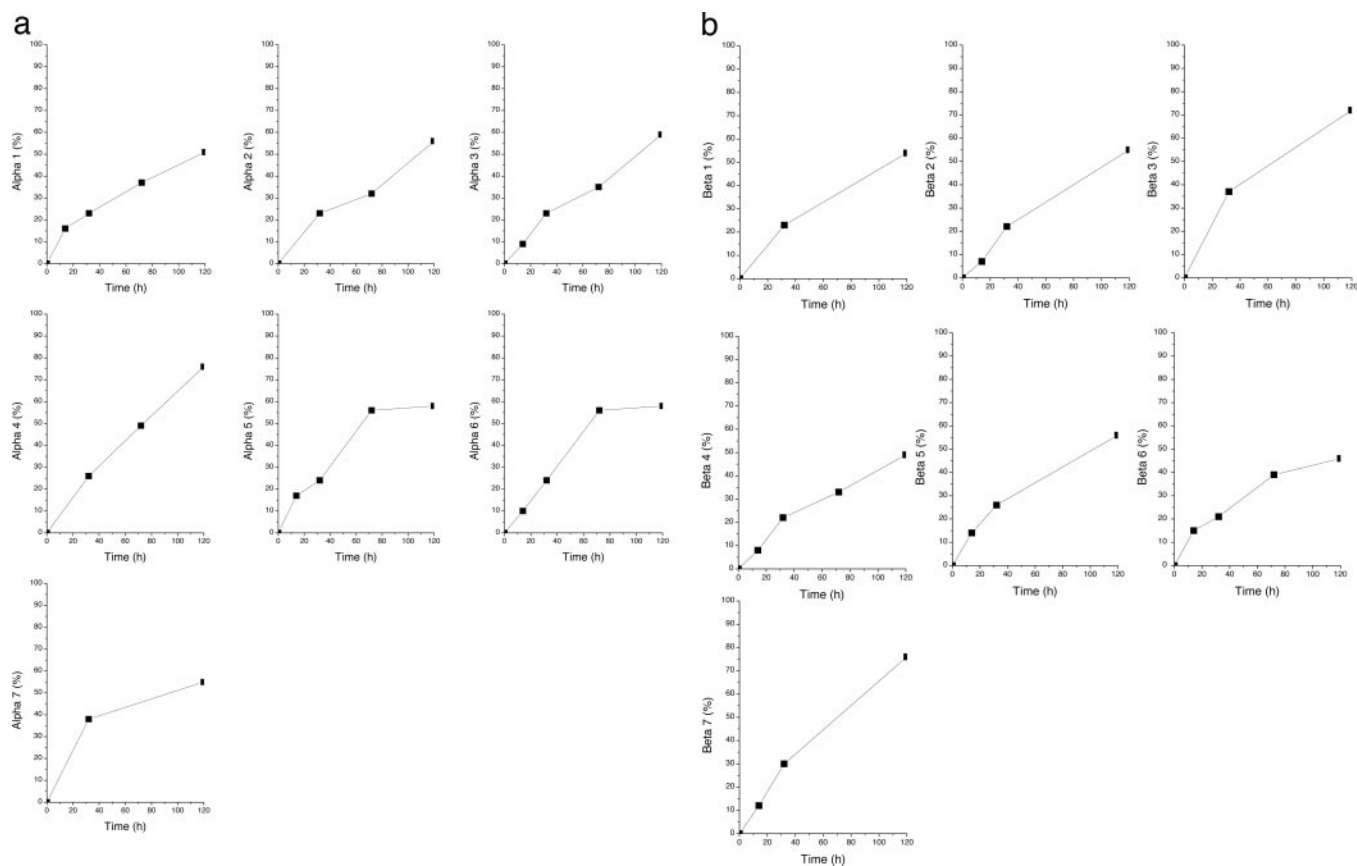


FIG. 8. Rate of synthesis for the 20S complex proteins calculated from heavy-light valine peptides. The turnover rate for each of the α and β subunits of the 20S proteasome was expressed as the percentage of newly synthesized protein over 0, 14, 32, 72, and 120 h.

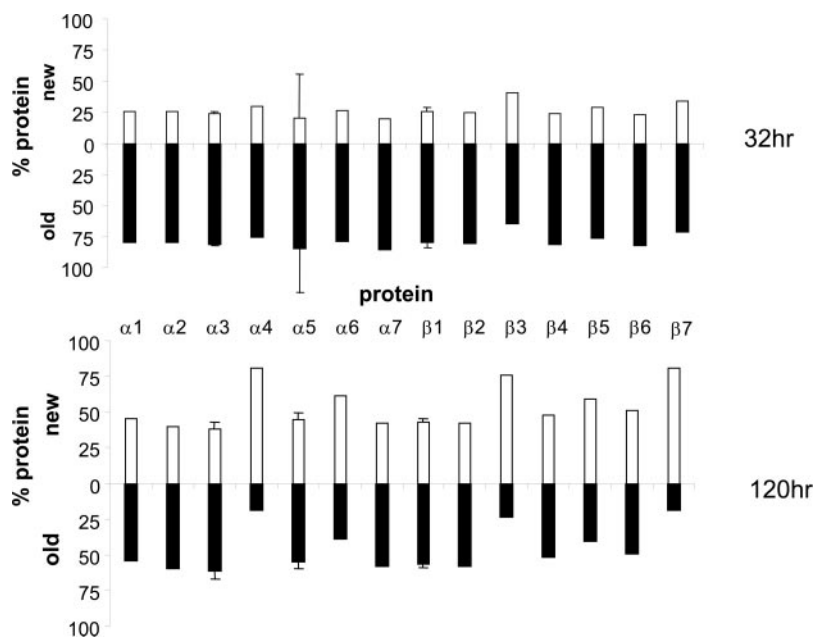
good signal-to-noise ratio and preferably isolated from other peaks. For most 20S subunits, it was possible to calculate relative turnover rates from monovaline peptides, but for subunits $\alpha 4$ and $\beta 2$ it was necessary to use divaline peptides, which requires a modified mathematical treatment (8). Some of the spectra obtained by MALDI-TOF had a relatively low total ion count, and few peptides were visible above the noise; this includes protein $\beta 3$. To overcome this limitation, we collected data over a narrow m/z range and accumulated spectra for over 2000 laser shots. The signal-to-noise ratio was greatly enhanced by this modification, allowing calculation of reliable turnover rates for these proteins. At 120 h, every subunit had incorporated sufficient label to allow clear identification of the H and L variants (Fig. 7). However, for this study, we have not attempted to calculate absolute turnover rates.

As the birds consumed the stable isotope-labeled diet, the ingested valine (at a RIA of 0.5) equilibrated with existing valine pools in the body. The true tissue RIA was calculated by MIDA, making use of peptides containing multiple valine residues as described in Ref. 8. Ultimately, the tissue RIA would be expected to attain the same value as the ingested valine, but over the limited labeling period here, up to 120 h, the precursor RIA reached a plateau value of 0.355 within 3.5 h and remained virtually unchanged thereafter (8). The pre-

plateau phase therefore made a minimal contribution to the total time integral of precursor labeling, and it was feasible to determine the degree of label incorporation into the different proteins within the 20S particle. Because each subunit was resolved by 2D gel electrophoresis, peptides containing a single valine were sought and used for measurement of incorporation.

At a precursor isotope abundance of 0.355 (35.5% heavy precursor), there was approximately a one in three chance that a valine residue incorporated into the nascent polypeptide chain was labeled with stable isotope. Even high turnover proteins, in which none of the original protein chain remained, would therefore generate spectra in which the intensity of the heavy peptide ion is approximately one-third of that of the light peptide ion. If the protein had a lower rate of turnover, the intensity of the light peak would be proportionately larger, reflecting a contribution to the light peak of previously synthesized, unlabeled material that is being degraded slowly. Knowledge of the precursor RIA and the intensity of the heavy peptide ion signal allows the corresponding ion intensity of the light peptide to be deconstructed into components corresponding to "new" and "old" protein, where "new" represents protein molecules synthesized during the labeling period and "old" reflects protein molecules remaining after degradation of pre-existing protein (8).

FIG. 9. **Relative turnover rates of 20S proteasome subunits.** For each of the 14 subunits, the relative turnover was expressed as the partition between pre-existing protein (*filled bars, old*) and newly synthesized protein (*open bars, new*) at 32 and 120 h of administration of [²H₃]valine. Where *error bars* are included, these reflect the fact that multiple valine-containing peptides could be analyzed to obtain replacement rates.



From this analysis, it is possible to define the rate of replacement of each of the 20S proteasome subunits. We have not attempted to compensate for the added protein as a result of tissue growth; this is relatively minor over the short labeling window, and within the proteasome all subunits are present at a rigidly fixed stoichiometry. Over 120 h, the synthesis of each subunit was very apparent as were differences in the overall rate of synthesis (Fig. 8). It is not possible at this stage to ascertain whether the turnover trajectories of the individual subunits are meaningful. Some labeling curves imply that the rate of synthesis is declining rapidly as the muscle develops; others are consistent with a sustained rate of synthesis. To summarize the data for each subunit, we include the partition between pre-existing material (old) and newly synthesized protein (new) in Fig. 9 at 32 and 120 h of labeling. A consistent pattern of behavior emerges. Although the rates of turnover of each of the subunits are maintained within a relatively narrow range, there was clear variance between subunits. For the α subunits, the relative rates of turnover are $\alpha_4 \gg \alpha_6 = \alpha_{1,2,3,5,7}$ and for the β subunits $\beta_3 = \beta_7 > \beta_5 > \beta_{1,2,4,6}$. The highest rate of replacement over 120 h is for subunit β_7 , such that 81% of the protein is replaced over this period. By contrast, other subunits are turned over at relatively low rates, of the order of 52% in 120 h for α_5 and β_4 . Because this analysis is based on the intact 20S proteasome, which maintains a strict stoichiometry of subunit composition, we infer from the differences in synthesis rates that some of the subunits are synthesized at higher rates than others and that there is some overproduction of subunits that, having failed to assemble into the mature 20S structure, are degraded rapidly. However, the data are also consistent with a model in which the proteasome undergoes partial disassembly and re-assembly. In such a model, newly synthesized subunits might exchange with pre-existing

subunits and demonstrate a higher rate of turnover (=replacement) within the complex. However, the latter model would not be consistent with our current view of proteasome biogenesis, including the irreversible step of zymogen activation. We therefore favor the alternative explanation that although demonstrating overall similar rates of synthesis, the proteasome is assembled from the pool of precursors such that surplus subunits are discarded and therefore that some subunits or subunit precursors are generated in rate-limiting quantities. These subunits may be key to controlling the rate of assembly of proteasome. Analysis of the rates of turnover of subunits within partially assembled intermediates may reveal these roles.

Acknowledgment—We thank Duncan Robertson for MS support.

* This work was supported by the Biotechnology and Biological Sciences Research Council. The costs of publication of this article were defrayed in part by the payment of page charges. This article must therefore be hereby marked “advertisement” in accordance with 18 U.S.C. Section 1734 solely to indicate this fact.

|| To whom correspondence should be addressed: Dept. of Veterinary Preclinical Sciences, University of Liverpool, Crown St., Liverpool L69 7ZJ, UK. Tel.: 44-151-794-4312; Fax: 44-151-794-4243; E-mail: r.beynon@liv.ac.uk.

REFERENCES

1. Baumeister, W., Walz, J., Zühl, F., and Seemüller, E. (1998) The proteasome: Paradigm of a self-compartmentalizing protease. *Cell* **92**, 367–380
2. Tanaka, K. (1998) Molecular biology of the proteasome. *Biochem. Biophys. Res. Commun.* **247**, 537–541
3. Zühl, F., Seemüller, E., Golbik, R., and Baumeister, W. (1997) Dissecting the assembly pathway of the 20S proteasome. *FEBS Lett.* **418**, 189–194
4. Groll, M., and Huber, R. (2003) Substrate access and processing by the 20S proteasome core particle. *Int. J. Biochem. Cell Biol.* **35**, 606–616
5. Jayarapu, K., and Griffin, T. A. (2004) Protein-protein interactions among human 20S proteasome subunits and proteasomblin. *Biochem. Biophys. Res. Commun.* **314**, 523–528

6. Rivett, A. J., Bose, S., Brooks, P., and Broadfoot, K. I. (2001) Regulation of proteasome complexes by γ -interferon and phosphorylation. *Biochimie* **83**, 363–366
7. Groettrup, M., Khan, S., Schwarz, K., and Schmidtke, G. (2001) Interferon-gamma inducible exchanges of 20S proteasome active site subunits: Why? *Biochimie* **83**, 367–372
8. Doherty, M. K., Whitehead, C., McCormack, H., Gaskell, S. J., and Beynon, R. J. (2004) Proteome dynamics in complex organisms: Using stable isotopes to monitor individual protein turnover rates. *Proteomics* **5**, 522–533
9. Beynon, R. J., Doherty, M., Hayter, J., El-Shafei, A., McLean, L., Robertson, D. H. R., and Gaskell, S. J. (2003) Protein turnover in chicken skeletal muscle: understanding protein dynamics on a proteome-wide scale. *Br. Poultry Sci.* **44**, Supp. 1, S9–S11
10. Doherty, M. K., McLean, L., Hayter, J. R., Pratt, J. M., Robertson, D. H. L., El-Shafei, A., Gaskell, S. J., and Beynon, R. J. (2004) The proteome of chicken skeletal muscle: Changes in soluble protein expression during growth in a layer strain. *Proteomics* **4**, 2082–2093
11. Taillandier, D., Combaret, L., Pouch, M. N., Samuels, S. E., Bechet, D., and Attaix, D. (2004) The role of ubiquitin-proteasome-dependent proteolysis in the remodelling of skeletal muscle. *Proc. Nutr. Soc.* **2004** **63**, 357–361
12. Dobby, A., Martin, S. A., Blaney, S. C., and Houlihan, D. F. (2004) Protein growth rate in rainbow trout (*Oncorhynchus mykiss*) is negatively correlated to liver 20S proteasome activity. *Comp. Biochem. Physiol. A. Mol. Integr. Physiol.* **137**, 75–85
13. Thomas, A. R., Oosthuizen, V., Naude, R. J., and Muramoto, K. (2002) Purification and characterization of the 20S proteasome from ostrich skeletal muscle. *Biol. Chem.* **383**, 1267–1270
14. Dahlmann, B., Kuehn, L., Rutschmann, M., and Reinauer, H. (1985) Purification and characterization of a multicatalytic high-molecular-mass proteinase from rat skeletal muscle. *Biochem. J.* **228**, 161–170
15. Tanaka, K., Kunio, I., and Ichihara, A. (1986) A high molecular weight protease in the cytosol of rat liver. I. Purification, enzymological properties, and tissue distribution. *J. Biol. Chem.* **261**, 15197–15203
16. Sawada, H., Muto, K., Fujimuro, M., Akaishi, T., Sawada, M. T., Yokosawa, H., and Goldberg, A. L. (1993) Different ratios in 20 S proteasomes and regulatory subunit complexes in two isoforms of the 26 S proteasome purified from rabbit skeletal muscle. *FEBS Lett.* **335**, 207–212
17. Shevchenko, A., Wilm, M., Vorm, O., and Mann, M. (1996) Mass spectrometric sequencing of proteins silver-stained polyacrylamide gels. *Anal. Chem.* **68**, 850–858
18. Perkins, D. N., Pappin, D. J., Creasy, D. M., and Cottrell, J. S. (1999) Probability-based protein identification by searching sequence databases using mass spectrometry data. *Electrophoresis* **20**, 3551–3567
19. Deleted in proof
20. Bose, S., Brooks, P., Mason, G. G., and Rivett, A. J. (2001) γ -Interferon decreases the level of 26 S proteasomes and changes the pattern of phosphorylation. *Biochem. J.* **353**, 291–297
21. Thomson, S., and Rivett, A. J. (1996) Processing of N3, a mammalian proteasome β -type subunit. *Biochem. J.* **315**, 733–738
22. Tokunaga, F., Aruga, R., Iwanaga, S., Tanaka, K., Ichihara, A., Takao, T., and Shimonishi, Y. (1990) The NH₂-terminal residues of rat liver proteasome (multicatalytic proteinase complex) subunits, C2, C3 and C8, are N α -acetylated. *FEBS Lett.* **263**, 373–375
23. Claverol, S., Burlet-Schiltz, O., Giralbal-Neuhauser, E., Gairin, J. E., and Monsarrat, B. (2002) Mapping and structural dissection of human 20 S proteasome using proteomic approaches. *Mol. Cell. Proteomics* **1**, 567–578
24. Kopp, F., Hendil, K. B., Dahlmann, B., Kristensen, P., Sobek, A., and Uerkvitz, W. (1997) Subunit arrangement in the human 20S proteasome. *Proc. Natl. Acad. Sci. U. S. A.* **94**, 2939–2944
25. Pratt, J. M., Petty, J., Riba-Garcia, I., Robertson, D. H. L., Gaskell, S. J., Oliver, S. G., and Beynon, R. J. (2002) Dynamics of protein turnover, a missing dimension in proteomics. *Mol. Cell. Proteomics* **1**, 579–591
26. Pratt, J. M., Robertson, D. H. L., Gaskell, S. J., Riba-Garcia, I., Hubbard, S. J., Sidhu, K., Oliver, S. G., Butler, P., Hayes, A., Petty, J., and Beynon, R. J. (2002) Stable isotope labelling *in vivo* as an aid to protein identification in peptide mass fingerprinting. *Proteomics* **2**, 157–163